PHYSICAL REVIEW A **80**, 023405 (2009)

Nondipole and interchannel-coupling effects in the photodetachment of Cl$^-$

J. Jose,[1] G. B. Pradhan,[1] P. C. Deshmukh,[1,*] V. Radojević,[1,2] and S. T. Manson[3]
[1]*Department of Physics, Indian Institute of Technology–Madras, Chennai 600 036, India*
[2]*Institute of Physics, Pregrevica 118, P.O. Box 68, 11080 Beograd-Zemun, Serbia*
[3]*Department of Physics and Astronomy, Georgia State University, Atlanta, Georgia 30303, USA*

(Received 21 April 2009; published 11 August 2009)

Nondipole photodetachment parameters for the $3p$ subshell of Cl$^-$ are calculated using relativistic random-phase approximation (RRPA). Interchannel-coupling effects on nondipole photodetachment parameters for the $3p$ subshell are studied with different degrees of truncation of the RRPA. It is inferred from the present investigations that the shape resonance in the photodetachment cross-section profile and the positions of the Cooper minima are sensitive to interchannel coupling. An analysis of the angular distribution of the photoelectrons reveals how the Cooper minima in the dipole and the quadrupole channels introduce a complex energy dependence, with peaks and zeroes, of the nondipole asymmetry parameter ζ.

DOI: 10.1103/PhysRevA.80.023405 PACS number(s): 32.80.Gc

I. INTRODUCTION

Photodetachment involves the removal of an electron from a negative ion by irradiating it with electromagnetic radiation, leaving the core neutral. Many-electron correlations are of greater significance in negative ions compared to that in neutral atoms because of the absence of a long-range Coulomb attraction. Part of the importance of photodetachment studies of negative ions is thus attributed to the significant insight into many-body effects obtained from investigation of the structure and transitions of these ions [1].

Structure calculations of atoms and ions have been of great interest in atomic physics. Resonant ionization spectroscopy (RIS) [2] and calculations using multiconfiguration Dirac- or Hartree-Fock theory [3] as well as many-body perturbation theory [4] are some of the methods which are used to investigate the ground state of negative ions. Near-threshold photodetachment studies lead to resonance structures which give greater insight into the excited states of these systems [5,6]. Alternative formalisms have been developed to describe the photoionization or photodetachment processes, such as many-body perturbation theory (MBPT) [7], *R*-matrix methods [8], multiconfiguration Dirac- or Hartree-Fock theory, [9] etc. The relativistic random-phase approximation (RRPA) [10] is one of the methods which takes into account important many-electron correlations and has been applied to address the photodetachment process in negative ions [11]. A formalism referred to as RRPA-R [12], which is based on the RRPA and takes into account the relaxation of the atomic core in the ionization process, is another method that has been successfully applied to negative ionic systems [13]. Photodetachment of the halogen ions and specifically investigations of many-body correlations in these systems are of great interest [11,13,14]. Measurements have been carried out to obtain the photodetachment parameters of halogen negative ions in low-energy regions [15–17]. Recently, we have employed the RRPA and RRPA-R methodologies to investigate the relaxation effects in the intermediate shells of Cl$^-$ and Br$^-$ [18]. It was concluded in this work that there exist significant relaxation effects near threshold. In addition, the combined effect of relaxation and core polarization, the latter introduced in an *ad hoc* manner, in valance photodetachment of Cl$^-$ has also been studied [19].

All of the photodetachment studies mentioned above have been carried out only in the dipole ($E1$) approximation which is generally believed to be applicable up to ~5 keV above the ionization threshold. However, high-precision instruments and bright light sources reveal higher-order multipole effects even at very low photon energies [20–22]. Effects of electron correlations on nondipole photoionization parameters for neutral atoms have been studied by employing interchannel coupling [23,24] at various levels of truncation of the RRPA. Near-threshold behavior of dipole and nondipole angular distribution asymmetry parameters of I$^-$ has been studied recently using Hartree-Fock (HF) and random-phase-approximation exchange (RPAE) methods [25].

Although RRPA photodetachment calculations in the dipole ($E1$) approximation on the negative chlorine ion (Cl$^-$,$Z=17$) have been reported earlier [11], we have repeated these $E1$ calculations in order to make explicit use of the dipole matrix elements (both magnitudes and phases) which are required for calculation of the nondipole photoelectron angular distribution; we have also carried out the quadrupole ($E2$) photodetachment calculations using the RRPA. We have investigated the effects of interchannel coupling on the shape resonance in the cross section and on the positions of the minima in quadrupole photodetachment matrix elements. By carrying out a detailed investigation of the matrix elements and the angular distribution of the photoelectrons, we deduce that the minima in the cross section are in fact the well-known Cooper minima [26] which are produced by the nodal behavior of the radial-wave functions of the electron in the initial states of photoionization or photodetachment. It is known that the dipole and nondipole photoelectron angular distribution asymmetry parameters show interesting dynamical effects due to interchannel coupling in the vicinity of the Cooper minima [23,24,27,28]. Measurements of the dipole angular distribution of photoelectrons resulting from the photodetachment of He$^-$ [29] manifest many-body effects in reasonable agreement with multicon-

---

[*] Corresponding author; pcd@physics.iitm.ac.in

TABLE I. Theoretical and experimental photodetachment thresholds of Cl^- in a.u. (27.21 eV).

Subshell	DHF	Experiment [31]
$3p_{3/2}$	0.1480	0.1329
$3p_{1/2}$	0.1532	0.1370
$3s_{1/2}$	0.7398	
$2p_{3/2}$	7.6762	
$2p_{1/2}$	7.7410	
$2s_{1/2}$	10.2981	

figuration Hartree-Fock (MCHF) calculations [30].

The theoretical framework that has been used in the present work is discussed briefly in Sec. II. The results are presented and discussed in Sec. III and conclusions are given in Sec. IV.

II. BRIEF DISCUSSION OF THEORY

Interchannel-coupling effects in Cl^- are studied in the present work by performing RRPA [10] calculations for both dipole and quadrupole photodetachments with various degrees of truncation. For the quadrupole ($E2$) case, the following combinations of channels were taken into account: six channels from the $3p$ subshell, eight channels from the $3p$ and $3s$ subshells, and 14 channels from the $3p$, $3s$, and $2p$ subshells. Similarly, for the dipole ($E1$) case, the channels that were coupled are five channels from the $3p$ subshell, seven channels from the $3p$ and $3s$ subshells, and 12 channels from the $3p$, $3s$, and $2p$ subshells.

The ground-state configuration of Cl^- is the same as that of the ground state of Ar. Dirac-Hartree-Fock (DHF) ground-state wave functions were used in the RRPA. The absolute values of the DHF orbital energy eigenvalues, which are the thresholds in the RRPA, are given in Table I, along with available experiment [31] where it is seen that DHF gives a reasonable result for the outer thresholds.

The general multipole transition matrix element between an initial ground-state orbital $n_b\kappa_b$ and an excited orbital $\epsilon\kappa$ is given by [32]

$$M_j^{(\lambda)}(\kappa,\kappa_b) = i^{-l+1} e^{i\delta_\kappa}\langle \epsilon\kappa \| q_j^{(\lambda)} \| n_b\kappa_b\rangle, \tag{1}$$

where δ_k is the phase shift, l is the orbital angular-momentum quantum number of the continuum state, and $q_j^{(\lambda)}$ is the multipole operator for the electromagnetic interaction, wherein $j=1$ for electric ($\lambda=1$) or magnetic ($\lambda=0$) dipole operators and $j=2$ for electric or magnetic-quadrupole operators. The electric dipole ($E1$) and quadrupole ($E2$) transition matrix amplitudes are usually denoted as $D_{\kappa\kappa_b}=M_1^{(1)}(\kappa,\kappa_b)$ and $Q_{\kappa'\kappa_b}=M_2^{(1)}(\kappa',\kappa_b)$.

The expression for the dipole cross section is [32]

$$\sigma_{E1}(\omega) = \frac{4\pi^2\alpha}{3}\omega\sum_{\kappa}|D_\kappa|^2 \tag{2}$$

and for the quadrupole cross section it is [27]

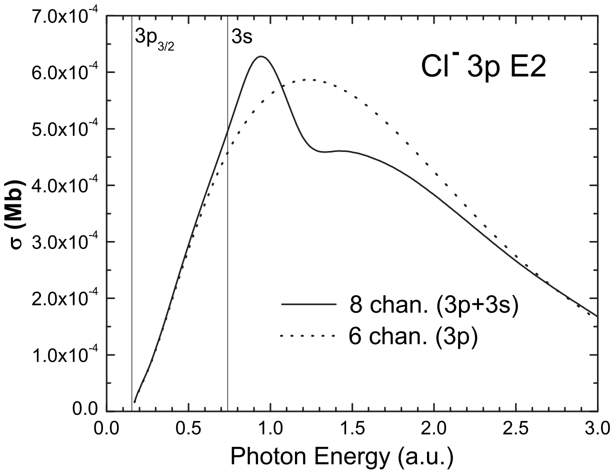

FIG. 1. Quadrupole ($E2$) cross section of the $3p$ shell of Cl^- for two levels of truncation of RRPA: channels from $3p+3s$, eight channels (solid line) and from $3p$, six channels (dotted line). Vertical lines indicate thresholds.

$$\sigma_{E2}(\omega) = \frac{4\pi^2\alpha^3}{60}\omega^3\sum_{\kappa}|Q_\kappa|^2, \tag{3}$$

where κ represents all possible dipole or quadrupole channels. The differential cross section for photodetachment or photoionization for linearly polarized incident photon is given by [33]

$$\frac{d\sigma}{d\Omega} = \frac{\sigma}{4\pi}[1 + \beta P_2(\cos\,\theta) + (\delta + \gamma\cos^2\,\theta)\sin\,\theta\cos\,\phi], \tag{4}$$

where σ is the total cross section including dipole and quadrupole contributions, β is the dipole photoelectron angular distribution asymmetry parameter (which arises from the interference between various dipole channels), δ and γ are the quadrupole angular distribution asymmetry parameters (which arise from interference between various electric-dipole and electric-quadrupole channels), and the angles θ and ϕ are the angles that the photoelectron direction makes with the photon polarization and the photon propagation, respectively. Using these formulae, the dipole and quadrupole photodetachment parameters have been calculated and the results are discussed in the next section.

III. RESULTS AND DISCUSSION

A. Interchannel-coupling effects on 3*p* quadrupole cross section in the region of shape resonance

The $E2$ cross section for the $3p$ shell is shown in Fig. 1 for two levels of truncation of the RRPA: for channels coming from the $3p$ shell only (six channels) and for channels from $3p$ and $3s$ shells (eight channels). Results for the 14-channel RRPA (inclusive of coupling with channels from the $2p$ subshells) are not shown since they are almost exactly the same as the eight-channel results. The ratio of $3p_{3/2}$ and $3p_{1/2}$ cross sections (branching ratio) is almost exactly equal to the

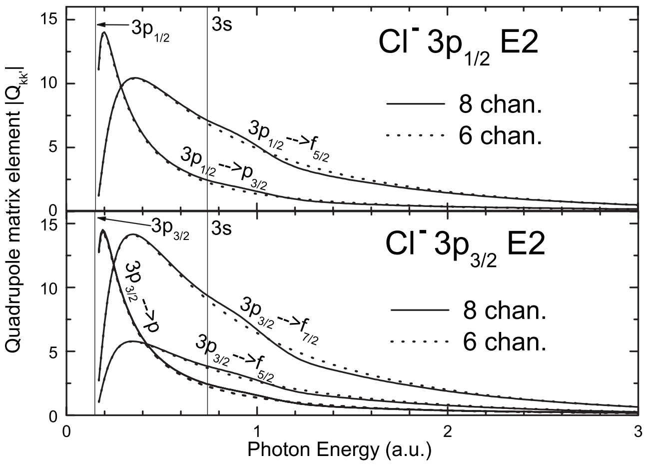

FIG. 2. Absolute values of the quadrupole ($E2$) matrix elements for the channels from $3p_{1/2}$ subshell (upper panel) and from the $3p_{3/2}$ subshell (lower panel). The respective solid line and dotted line represent matrix elements of eight-channel and six-channel calculations. The matrix elements of the channels $3p_{3/2}\rightarrow p_{3/2}$ and $3p_{3/2}\rightarrow p_{1/2}$ are almost identical so that the transition is designated only as $3p_{3/2}\rightarrow p$. Vertical lines indicate thresholds.

statistical value of 2 and, hence, the individual partial cross sections of the $3p_{1/2}$ and $3p_{3/2}$ subshells are not shown. As seen in this figure, interchannel coupling between $3p$ and $3s$ photodetachment channels induces considerable alteration of the shape resonance. The maximum of the cross section of the six-channel calculation shifts significantly due to interchannel coupling. Also, coupling with the $3s$ channels causes a local dip in the eight-channel $3p$ $E2$ photodetachment cross section at ~ 1.2 a.u.

In order to understand these features in some detail, the six- and eight-channel quadrupole matrix elements for $3p_{1/2}$ and $3p_{3/2}$ subshells are shown in Fig. 2. The shape resonance in the quadrupole $p\rightarrow f$ transition is clearly seen in Fig. 2. Generally, however, when cross sections are significantly affected by interchannel coupling, these interchannel effects show up in the transition matrix elements as well. This is well-known in dipole photoionization and several results in the quadrupole case have also been shown. The present case is different in that the energy dependence of the matrix elements themselves, calculated with and without coupling of the $3p$ and $3s$ channels, does not show much difference (Fig. 2), but the cross section shows a significant effect (Fig. 1). The minor difference in the six-channel and the eight-channel truncated RRPA matrix elements of Fig. 2 gets magnified by the ω^3 factor in the expression for the $E2$ cross section resulting in the interchannel-coupling effect in the cross section, displayed in Fig. 1.

Of course, this quadrupole cross section is 3 or 4 orders of magnitude smaller than the dipole cross section and, thus, is not observable over the dipole background. The result is shown simply to counter the notion that correlation effects are generally unimportant in the quadrupole channel [32]. In addition, the effects could well be modified by relaxation and/or polarization effects that are not included in the present calculation. Nevertheless, the effects of relaxation and polarization cannot obliterate the existence of correlation in the form of interchannel coupling.

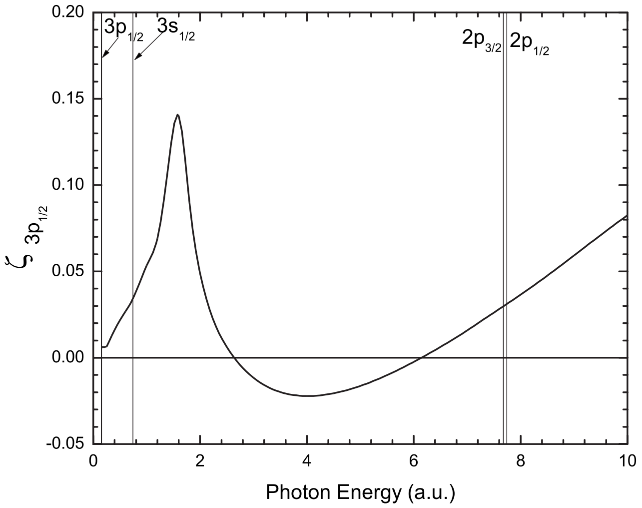

FIG. 3. Nondipole angular distribution asymmetry parameter $\zeta_{3p_{1/2}}$. Vertical lines indicate thresholds.

B. Photoelectron angular distribution near Cooper minima

It is convenient to look at the nondipole contribution to the photoelectron angular distribution in terms of another related parameter, $\zeta=\gamma+3\delta$, in order to exploit the geometrical angular distribution of photoelectrons in an experimental setup which makes use of three time-of-flight analyzers in order to identify the nondipole contributions [22]. Figure 3 shows this parameter ζ for the $3p_{1/2}$ subshell of Cl^-. The $3p_{3/2}$ is almost exactly the same so it is not shown; we focus on $3p_{1/2}$ because it is simpler to analyze owing to the fact that there are fewer channels contributing to the photodetachment than in the case of $3p_{3/2}$. The principal features seen in this figure are (a) ζ peaks near photon energy of ~ 1.6 a.u., (b) ζ goes to a zero near photon energy of ~ 2.7 a.u., and (c) also near ~ 6.2 a.u.

To aid in analyzing the behavior of ζ, we express ζ [22,32] as a sum of four terms, each of which represents a contribution from the interference of a single dipole channel with a single quadrupole channel. Then, designating the dipole transitions and the quadrupole transitions from $np_{1/2}$, respectively, by index κ and κ', then each of the interference term which contributes to $\zeta_{np_{1/2}}$ has the form

$$a_{\kappa,\kappa'} = (-1)^{(j+j')}\frac{k}{\bar{\sigma}}\left(-\frac{2\sqrt{105}}{5}A_3+\frac{9\sqrt{30}}{10}A_1\right)|D_{\kappa,\kappa_b}| \times |Q_{\kappa',\kappa_b}|\cos\Delta_{\kappa,\kappa'}, \tag{5}$$

where

$$A_l = (-1)^{(j'+j_b)}\langle\kappa'\|C_l\|\kappa\rangle\begin{Bmatrix} 1 & 2 & l \\ j' & j & j_b \end{Bmatrix} \tag{6}$$

and $\bar{\sigma}$ is the sum of the dipole and the quadrupole cross section divided by $\frac{4\pi^2\alpha}{3}\omega$—the reduced cross section. Since there are two dipole and two quadrupole channels coming from excitations of $3p_{1/2}$ subshell, there are four such terms and, for convenient analysis, we express the angular distribution asymmetry parameter ζ as

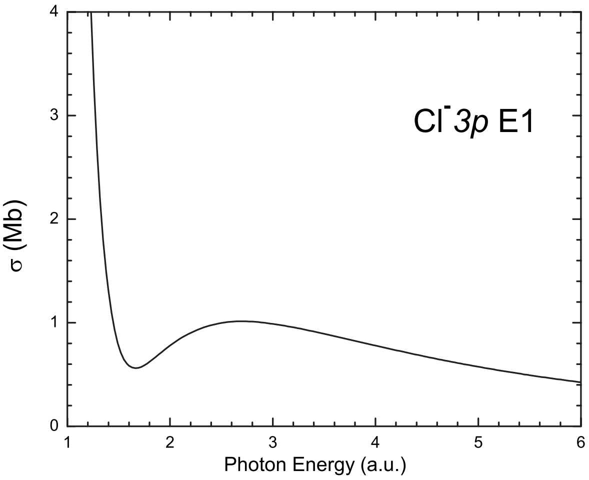

FIG. 4. Dipole cross section of the $3p$ subshell in the Cooper minimum region [11].

$$\zeta_{3p_{1/2}} = \sum_{\kappa,\kappa'} a_{\kappa,\kappa'}, \qquad (7)$$

where $\kappa=-1,2$, $\kappa'=-2,3$, and $\kappa_b=1$.

As seen from Eqs. (5) and (7), the expression for ζ has in the denominator the total sum of the reduced dipole and quadrupole cross sections. Since the dipole cross section is much larger than the quadrupole, the denominator $\bar{\sigma}$ is determined almost entirely by the dipole cross section, so that the expression for ζ becomes, to an excellent approximation, a weighted sum of ratios of quadrupole to dipole matrix elements. It is known that the Cooper minimum in each of the $3p \rightarrow d$ dipole channels is located at ~1.6 a.u. photon energy [11], causing the denominator in the expression for ζ to decrease, thereby resulting in an increase in ζ; this explains the maximum in ζ seen in Fig. 3. The calculated Cooper minimum in the $3p$ dipole cross section which causes peak in ζ is shown Fig. 4 and this result reproduces the result of Ref. [11].

The zero in ζ near photon energy ~6.2 a.u. is due to the quadrupole Cooper minimum in the $3p_{1/2}$ cross section, seen in Fig. 5 at the various levels of truncation of the RRPA. It is evident that the exact location of the Cooper minimum is slightly sensitive to the actual channels coupled in the truncated RRPA calculations. The matrix elements which contribute to the $3p_{1/2}$ $E2$ cross section are shown in Fig. 6, for the case of 14 $E2$ channels coupled, and clearly show the Cooper minimum in the quadrupole channel $3p_{1/2} \rightarrow \epsilon f_{5/2}$ near photon energy ~6 a.u. This minimum in the $3p_{1/2} \rightarrow \epsilon f_{5/2}$ channel causes the terms $a_{-1,3}$ and $a_{2,3}$ to become vanishingly small at the energy of the quadrupole Cooper minimum. However, owing to the effect(s) of the two remaining terms in the expression for ζ, $a_{-1,-2}$ and $a_{2,-2}$, which are usually relatively unimportant except in the vicinity of a Cooper minimum, the energy at which $\zeta=0$ is not exactly the quadrupole Cooper minimum energy, but is rather close to it. This is clear from Fig. 7 in which the individual contributions $a_{\kappa,\kappa'}$ which add up to ζ, Eq. (7), are shown. Thus, the zero in ζ around 6 a.u. is due to a quadrupole Cooper minimum, but the zero is not exactly at the energy of the minimum.

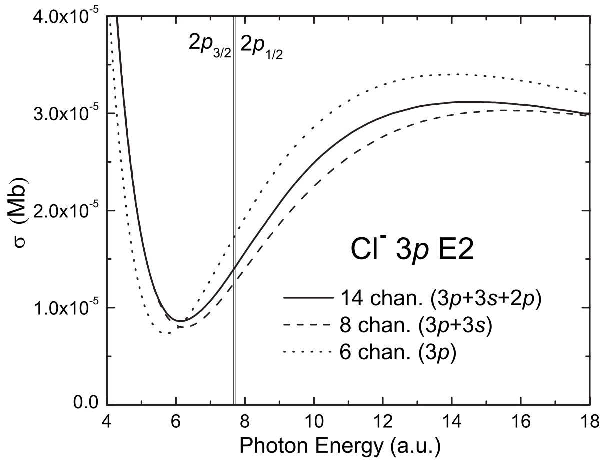

FIG. 5. Comparison of cross section of $3p$ shell for various degrees of truncations at higher energy. Solid line represents the result of the 14-channel calculation, dashed line represents that of eight-channel calculation, and dotted line that of six-channel calculation. Vertical lines indicate thresholds.

To check that $a_{-1,3}$ and $a_{2,3}$ attain a value ~0 because of the quadrupole Cooper minimum in the $3p_{1/2} \rightarrow \epsilon f_{5/2}$ matrix element, the remaining factors in the expression for $a_{\kappa,\kappa'}$, the dipole matrix elements, and the cos Δ must be investigated. The cosines of the phase-shift differences are given in Fig. 8 and it is evident that neither of the cos Δ terms has a zero at photon energy of ~6 a.u. This confirms that the zero in $\zeta_{3p_{1/2}}$ at ~6.2 a.u. is in fact due to the $E2$ Cooper minimum in the $3p_{1/2} \rightarrow \epsilon f_{5/2}$ matrix element.

And what of the zero in ζ near photon energy of ~2.7 a.u.? Our analysis shows that this zero in ζ is not due to a quadrupole Cooper minimum. It turns out that it is due to an accidental cancellation of the four contributing terms, $a_{\kappa,\kappa'}$, in the expression for ζ. Accordingly, we refer to such a

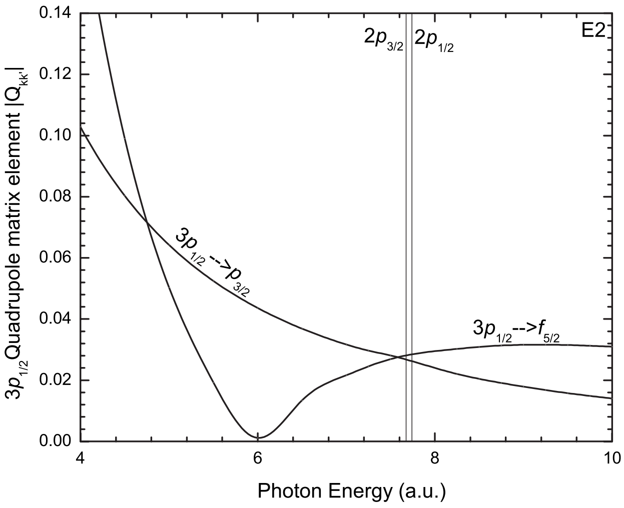

FIG. 6. Absolute values of the matrix elements which contribute to quadrupole ($E2$) cross section for $3p_{1/2}$. Vertical lines indicate thresholds.

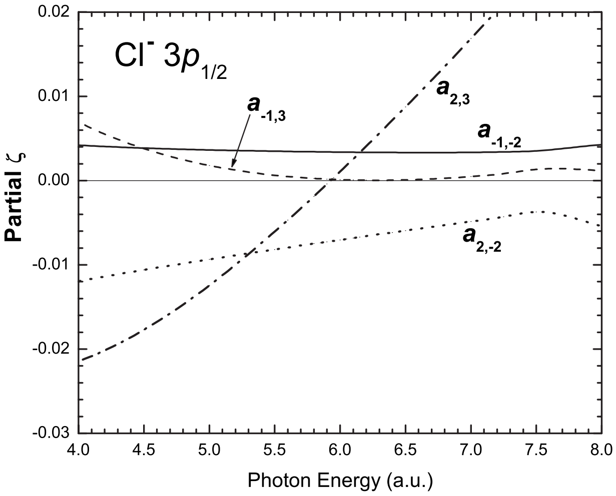

FIG. 7. Terms in expression for $\zeta_{3p_{1/2}}$, Eq. (7), with appropriate sign so that sum of these terms yields $\zeta_{3p_{1/2}}$.

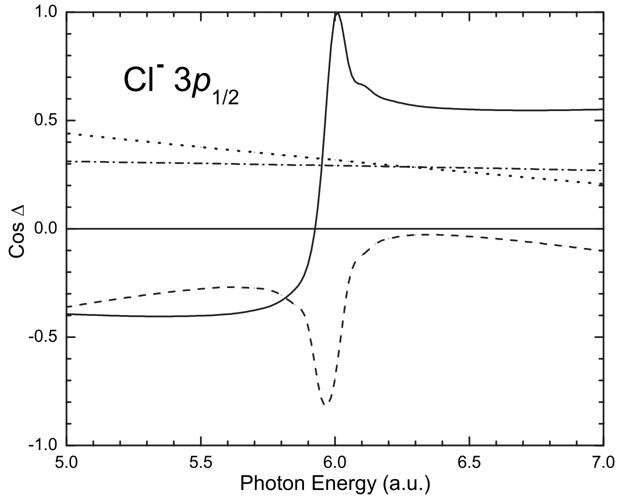

FIG. 8. cos Δ, the cosine of the phase-shift difference between $E1$ and $E2$ channels, as a function of photon energy. Solid line corresponds to $\delta E1(p_{1/2}\rightarrow d_{3/2})-\delta E2(p_{1/2}\rightarrow f_{5/2})$, dashed line corresponds to $\delta E1(p_{1/2}\rightarrow s_{1/2})-\delta E2(p_{1/2}\rightarrow f_{5/2})$, dotted line corresponds to $\delta E1(p_{1/2}\rightarrow d_{3/2})-\delta E2(p_{1/2}\rightarrow p_{3/2})$, and dash-dotted line corresponds to $\delta E1(p_{1/2}\rightarrow s_{1/2})-\delta E2(p_{1/2}\rightarrow p_{3/2})$.

case as an accidental zero. This means that, as a general rule, a quadrupole Cooper minimum leads to a zero in the ζ parameter, but a zero in ζ does not necessarily imply a quadrupole Cooper minimum.

Although the present calculations do not include relaxation or polarization, we believe that the results for ζ are reasonably accurate. This is because angular distribution parameters, unlike cross sections, are *ratios* of matrix elements. Now, the major effect of these omitted corrections is a reduction of the matrix elements owing to the overlap integrals that are less than unity owing to relaxation. But, since ζ is a ratio, these overlap integrals drop out. Thus, the calculated angular distribution parameters should be very much more accurate than the cross sections.

It is important to note that experimental techniques have reached a point that ζ parameters as small as 0.05 have been observed [28] so that the ζ parameter for the 3p subshell of Cl⁻ should be entirely measurable. In addition, the vanishing of ζ engendered by the quadrupole Cooper minimum near photon energy ~6.2 a.u. should also be seen experimentally, thereby providing another experimental verification of the existence of quadrupole Cooper minima.

IV. FINAL REMARKS

The present studies reveal that interchannel-coupling effects are present in the photodetachment cross section of 3p subshell of Cl⁻. These effects manifest most dramatically in the vicinity of the shape resonance in the cross section. At higher energies, it is found that the exact location of the quadrupole Cooper minimum depends on the level of truncation of the RRPA, thus demonstrating the sensitivity of the position of the Cooper minimum to interchannel coupling. It is therefore important to include the effect of electron correlations in photodetachment studies. Furthermore, from the present studies, it is concluded that Cooper minima in the dipole channels and quadrupole channels very strongly affect the nondipole photoelectron angular distribution asymmetry parameter ζ with a peak around the dipole Cooper minimum and a zero near quadrupole Cooper minimum. In addition, it was found that cancellation among the various contributions to the ζ parameter could also result in a zero in ζ. Note further that these observations should be general and apply to any subshell of any ion or atom, particularly those which exhibit dipole or quadrupole Cooper minima. Finally, it is to be emphasized that, given the magnitude of ζ, it appears that Cl⁻ is an excellent case for experimental scrutiny of quadrupole Cooper minima.

ACKNOWLEDGMENTS

We are very grateful to Professor W. R. Johnson for sustained help in these studies and for the use of the primary codes employed in the present work. This work has been partially supported by the Department of Science and Technology, Government of India, and an international grant jointly sponsored by the Department of Science and Technology (India) and the National Science Foundation (USA). V.R. is supported in part by the Ministry of Science of the Republic of Serbia through Project No. 141029. Besides, V.R. acknowledges the support of IIT-Madras for the hospitality during his visit when this work was carried out. S.T.M. acknowledges the partial support of DOE, Division of Chemical Sciences.

---

[1] V. K. Ivanov, J. Phys. B **32**, R67 (1999); Radiat. Phys. Chem. **70**, 345 (2004).

[2] V. V. Petrunin, J. D. Voldstad, P. Balling, P. Kristensen, T. Andersen, and H. K. Haugen, Phys. Rev. Lett. **75**, 1911 (1995).

[3] S. M. O' Malley and D. R. Beck, Phys. Rev. A **77**, 012505 (2008).

[4] V. A. Dzuba and G. F. Gribakin, Phys. Rev. A **55**, 2443 (1997).

[5] G. Yu. Kashenock and V. K. Ivanov, J. Phys. B **39**, 1379 (2006).

[6] C. W. Walter, N. D. Gibson, C. M. Janczak, K. A. Starr, A. P. Snedden, R. L. Field III, and P. Andersson, Phys. Rev. A **76**, 052702 (2007).

[7] R. L. Chase and H. P. Kelly, Phys. Rev. A **6**, 2150 (1972).

[8] N. Berrah, R. C. Bilodeau, I. Dumitriu, J. D. Bozek, N. D. Gibson, C. W. Walter, G. D. Ackerman, O. Zatsarinny, and T. W. Gorczyca, Phys. Rev. A **76**, 032713 (2007).

[9] C. Froese Fischer and J. E. Hansen, Phys. Rev. A **44**, 1559 (1991).

[10] W. R. Johnson and C. D. Lin, Phys. Rev. A **20**, 964 (1979); W. R. Johnson, C. D. Lin, K. T. Cheng, and C. M. Lee, Phys. Scr. **21**, 409 (1980).

[11] V. Radojević, H. P. Kelly, and W. R. Johnson, Phys. Rev. A **35**, 2117 (1987).

[12] V. Radojević, M. Kutzner, and H. P. Kelly, Phys. Rev. A **40**, 727 (1989).

[13] M. Kutzner, J. T. Brown, and J. Thorarinson, Phys. Rev. A **68**, 042713 (2003).

[14] V. Radojević and H. P. Kelly, Phys. Rev. A **46**, 662 (1992).

[15] A. Mandl, Phys. Rev. A **3**, 251 (1971).

[16] A. Mandl and H. A. Hyman, Phys. Rev. Lett. **31**, 417 (1973).

[17] A. Mandl, Phys. Rev. A **14**, 345 (1976).

[18] V. Radojević, J. Jose, G. B. Pradhan, P. C. Deshmukh, and S. T. Manson, Can. J. Phys. **87**, 49 (2009).

[19] M. Kutzner, J. A. Robertson, and P. Pelley, Phys. Rev. A **62**, 062717 (2000).

[20] O. Hemmers, R. Guillemin, E. P. Kanter, B. Krassig, D. W. Lindle, S. H. Southworth, R. Wehlitz, J. Baker, A. Hudson, M. Lotrakul, D. Rolles, W. C. Stolte, I. C. Tran, A. Wolska, S. W. Yu, M. Ya. Amusia, K. T. Cheng, L. V. Chernysheva, W. R. Johnson, and S. T. Manson, Phys. Rev. Lett. **91**, 053002 (2003).

[21] N. L. S. Martin, D. B. Thompson, R. P. Bauman, C. D. Caldwell, M. O. Krause, S. P. Frigo, and M. Wilson, Phys. Rev. Lett. **81**, 1199 (1998).

[22] O. Hemmers, G. Fisher, P. Glans, D. L. Hansen, H. Wang, S. B. Whitfield, R. Wehlitz, J. C. Levin, I. A. Sellin, R. C. C. Perera, E. W. B. Dias, H. S. Chakraborty, P. C. Deshmukh, S. T. Manson, and D. W. Lindle, J. Phys. B **30**, L727 (1997).

[23] P. C. Deshmukh, T. Banerjee, K. P. Sunanda, and H. R. Varma, Radiat. Phys. Chem. **75**, 2211 (2006).

[24] T. Banerjee, P. C. Deshmukh, and S. T. Manson, Phys. Rev. A **75**, 042701 (2007).

[25] M. Ya. Amusia, A. S. Baltenkov, L. V. Chernysheva, Z. Felfli, and A. Z. Msezane, Phys. Rev. A **72**, 032727 (2005).

[26] J. W. Cooper, Phys. Rev. **128**, 681 (1962).

[27] O. Hemmers, R. Guillemin, D. Rolles, A. Wolska, D. W. Lindle, K. T. Cheng, W. R. Johnson, H. L. Zhou, and S. T. Manson, Phys. Rev. Lett. **93**, 113001 (2004).

[28] P. C. Deshmukh, T. Banerjee, H. R. Varma, O. Hemmers, R. Guillemin, D. Rolles, A. Wolska, S. W. Yu, D. W. Lindle, W. R. Johnson, and S. T. Manson, J. Phys. B **41**, 021002 (2008).

[29] J. S. Thompson, D. J. Pegg, R. N. Compton, and G. D. Alton, J. Phys. B **23**, L15 (1990).

[30] D. S. Kim, H. L. Zhou, and S. T. Manson, Phys. Rev. A **55**, 414 (1997).

[31] B. M. Smirnov, *Negative Ions* (McGraw-Hill, New York, 1982).

[32] A. Derevianko, W. R. Johnson, and K. T. Cheng, At. Data Nucl. Data Tables **73**, 153 (1999).

[33] J. W. Cooper, Phys. Rev. A **47**, 1841 (1993).